Published in final edited form as:
Dev Neurosci. 2012 ; 34(4): 327–341. doi:10.1159/000341119.

Subcortical and Cortical Structural Central Nervous System Changes and Attention Processing Deficits in Preschool-Aged Children with Prenatal Methamphetamine and Tobacco Exposure

Chris Derauf[a], **Barry M. Lester**[b], **Nurunisa Neyzi**[c], **Minal Kekatpure**[c], **Luis Gracia**[c], **James Davis**[d], **Kalpana Kallianpur**[d], **Jimmy T. Efird**[e], and **Barry Kosofsky**[c]

[a]Mayo Clinic, Rochester, Minn

[b]The Warren Alpert Medical School at Brown University and Women and Infants Hospital, Providence, R.I

[c]Weill Cornell Medical College, New York, N.Y

[d]University of Hawaii, Honolulu, Hawaii

[e]Brody School of Medicine, Greenville, N.C., USA

Abstract

Objective—To examine the independent contributions of prenatal methamphetamine exposure (PME) and prenatal tobacco exposure (PTE) on brain morphology among a sample of nonalcohol-exposed 3- to 5-year-old children followed prospectively since birth.

Study Design—The sample included 20 children with PME (19 with PTE) and 15 comparison children (7 with PTE), matched on race, birth weight, maternal education and type of insurance. Subcortical and cortical volumes and cortical thickness measures were derived through an automated segmentation procedure from T1-weighted structural magnetic resonance images obtained on unsedated children. Attention was assessed using the computerized Conners' Kiddie Continuous Performance Test Version 5 (K-CPT™ V.5). PME effects on subcortical and cortical brain volumes and cortical thickness were tested by general linear model with type III sum of squares, adjusting for PTE, prenatal marijuana exposure, age at time of scan, gender, handedness, pulse sequence and total intracranial volume (for volumetric outcomes). A similar analysis was done for PTE effects on subcortical and cortical brain volumes and thickness, adjusting for PME and the above covariates.

Results—Children with PME had significantly reduced caudate nucleus volumes and cortical thickness increases in perisylvian and orbital-frontal cortices. In contrast, children with PTE showed cortical thinning in perisylvian and lateral occipital cortices and volumetric increases in frontal regions and decreases in anterior cingulate. PME was positively related and caudate volume was inversely related to K-CPT reaction time by inter-stimulus interval, a measure of the

Chris Derauf, MD, Department of Pediatric and Adolescent Medicine, Mayo Clinic, Rochester, MN 55905 (USA), Tel. +1 507 284 5243, derauf.donald@mayo.edu.

ability to adjust to changing task demands, suggesting that children with PME may have subtle attentional deficits mediated by caudate volume reductions.

Conclusions—Our results suggest that PME and PTE may have distinct differential cortical effects on the developing central nervous system. Additionally, PME may be associated with subtle deficits in attention mediated by caudate volume reductions.

Keywords

Prenatal drug exposure; Neuroimaging; Cognitive development; Attention

Introduction

Prenatal methamphetamine exposure (PME) is an important public health problem, with recent estimates suggesting a 5% prevalence rate in regions with endemic use [1]. Like cocaine, methamphetamine (MA) is a psycho-stimulant that blocks dopamine, norepinephrine and serotonin reuptake, increasing concentrations of these neurotransmitters in the synaptic cleft [2]. MA also enhances release of these neurotransmitters, inhibits monoamine oxidase and causes maternal vasoconstrictive and anorectic effects [3]. PME may additionally impact widespread neuroontogenic processes, such as cell production and migration [4], alter development of the fetal stress response axis [5], and perturb oxidative, mitochondrial and glutamate-associated excitotoxic pathways leading to neuronal damage [6].

In well-controlled prospective research, PME has been linked to deficits in fetal growth [7], to effects on infant arousal regulation, stress reactivity, motor control [8, 9], increased externalizing behavior problems at ages 3 and 5 [10], and to subtle deficits among 5-year-old children in inhibitory control [11], a key executive function (EF).

Neuroimaging studies of community-derived convenience samples of PME have identified neurocognitive deficits in specific EFs such as inhibitory control, working memory, sustained attention and visual-motor integration, along with volumetric changes in frontal-striatal brain regions important in regulating these functions. For example, Chang et al. [12] found smaller globus pallidus, putamen and hippocampal volumes, and borderline smaller caudate volumes in children with PME, while Sowell et al. [13] found volume reductions in the striatum, thalamus, parietooccipital and anterior prefrontal cortices, and volume increases in the anterior and posterior cingulate, ventral and medial temporal, and perisylvian cortices. However, data collected from these convenience samples may be subject to recall bias and selection bias, both of which can result in overestimates of negative outcomes [14]. Additionally, conclusions about the effects of PME on brain development may be confounded by the high rates of polydrug exposure, particularly alcohol and nicotine in exposed women [15]. For instance, prenatal alcohol exposure has been associated with decreased cortical, subcortical and cerebellar volumes [16], and with both decreased [17] and increased cortical thickness [18]. Likewise, neuroimaging studies of prenatal tobacco exposure (PTE) have identified cortical thinning among exposed participants in orbitofrontal, middle frontal and parahippocampal cortices [19]. In convenience samples, these confounding exposures, if inadequately documented or

underreported, along with the above biases, may result in the misattribution of effects. Therefore, to the greatest extent possible, neuroimaging studies of prenatal exposure should ideally both accurately identify and statistically adjust or stratify for coexposure to other drugs of abuse.

The purpose of this study was to examine the independent contributions of PME and PTE on structural brain development, which we pursued using FreeSurfer, a computer-assisted whole-brain MRI morphometric analysis pipeline which we adapted for use with a validated pediatric brain atlas [20]. We analyzed MR data sets and behavioral measures from a sample of nonalcohol-exposed 3- to 5-year-old children followed prospectively since birth in the largest federally funded prospective study of PME and child development, the Infant Development, Environment and Lifestyle (IDEAL) study.

Methods

Study Design

This is a cross-sectional neuroimaging study of preschool-aged children enrolled since birth in the Hawaii-site of the IDEAL study, currently being conducted at five clinical sites: the University of California, Los Angeles; the University of Hawaii; Blank Children's Hospital – Iowa Health, and the Universities of Oklahoma and Tulsa. Detailed recruitment methods for the IDEAL study have been reported previously [1, 21]. Briefly, between September 2002 and November 2004, all women delivering newborns at the above sites were approached, screened for eligibility and consented to participate. Maternal exclusions were: non-English speaking; <18 years of age; used opiates, LSD, PCP, or cocaine only during pregnancy; institutionalized for retardation or emotional disorders; low cognitive functioning, or current or past psychosis. Infant exclusions were: critically ill and unlikely to survive; multiple gestation; life-threatening congenital anomaly; chromosomal abnormality associated with mental or neurological deficiency; overt clinical evidence of an intrauterine infection, or sibling previously enrolled in the study. 34,833 mother-infant pairs were initially screened for enrollment, of which 17,961 (52%) were eligible for the study. Of these eligible participants, 3,705 (21%) consented to participate. At recruitment, sociodemographic and substance use information was collected by maternal interviews. Meconium samples were collected from all infants and analyzed by a central laboratory (US Drug Testing Laboratory, Des Plaines, Ill., USA) for drug metabolites. MA exposure was determined by standardized maternal self-report at birth and at the 1-month visit and/or a positive meconium screen with gas chromatography/mass spectroscopy confirmation. For longitudinal follow-up, MA-exposed infants and mothers (n = 204) were matched to unexposed comparison infant-mother pairs (n = 208) who denied MA use and had a negative meconium screen for MA. The two groups were matched on maternal race, birth weight category (<1,500, 1,500–2,500, >2,500 g), private versus public insurance, and education (high school education completed vs. not completed). Prenatal exposure to alcohol, tobacco and marijuana existed in both groups and were considered as background variables. Follow-up assessments were conducted at 1, 12, 24, 30, 36, 60 and 66 months of age.

Participants

This study evaluated MRI structural brain outcomes among study participants assessed between the ages of 3 and 5 years. Only Hawaii-site IDEAL study participants without a history of prenatal alcohol exposure were eligible given its well-known teratogenic effects on the developing central nervous system (CNS). 120 children of the total Hawaii IDEAL cohort of 153 children met this exclusion. Additional exclusion criteria included the presence of implanted metallic objects and any medical or psychological condition that would preclude MR imaging. Children were recruited after parent/guardian informed consent was received. Institutional review board approval was obtained from the University of Hawaii and the Queens Medical Center, both in Honolulu, Hawaii, and the study included a federal certificate of confidentiality. Of the eligible 120 children, 64 (53.3%) were consented to participate and 43 (33.3%) attempted or underwent MR imaging on one or more occasions. Of these, 8 children, 3 PME and 5 non-PME, were either unable to be acclimatized to the MRI or had excessive head movement resulting in poor quality images. Thirty-five (29.2%) had analyzable brain imaging data, 20 (57.1%) with PME and 26 (74.3%) with PTE.

Structural MRI Acquisition and Data Analysis

Structural brain images were acquired using the volumetric magnetization-prepared rapid gradient echo (MPRage) T1-weighted sequence run on a 3T Siemens Tim Trio scanner (Siemens Medical Solutions, Erlangen, Germany). Children were acclimatized to the scanner environment and provided a DVD movie of their choice to watch during scanning. No sedation was used. Total scan time was approximately 20–25 min. The majority of participants [PME = 17/20 (85%) vs. non-PME = 12/15 (80%)] were scanned using the following MPRage pulse sequence: TR = 2,200 ms, TE = 4.91 ms, TI = 1,000 ms, flip angle = 12°, field of view = 256 × 256 mm^2, slice thickness = 1 mm, resolution = 1 × 1 × 1 mm. Three PME and three non-PME participants were scanned using a modified MPRage pulse sequence: TR = 2,530 ms, TE = 3.33 ms, TI = 1,100 ms, flip angle = 7°, field of view = 256 × 256 mm^2, slice thickness = 1 mm, resolution = 1 × 1 × 1 mm. Two members of the research team (C.D. and K.K.) reviewed each MRI and excluded data sets with significant motion artifact from subsequent analysis. A neuroradiologist who was not involved in the research protocol provided a clinical reading of each scan.

To reconstruct brain morphological features, the 3D MPRAGE data were processed via the FreeSurfer software package v4.0.5 (http://surfer.nmr.mgh.harvard.edu) [22-24], using an automated pipeline custom developed for an XNAT-based DICOM-server hosted at Weill Cornell Medical College of Cornell University (https://ped-birn.med.cornell.edu/xnat/). Scans were corrected for motion, normalized for intensity and skull-stripped using the FreeSurfer software package. Subcortical volumes were derived by automated segmentation using a validated pediatric atlas [20]. This automated segmentation technique assigns a neuroanatomical label to each voxel on the image. The probability of each voxel being assigned a certain label depends upon both participant-specific measures of image intensity and spatial information, and participant-independent measures derived from the probabilistic atlas. For cortical and subcortical volumes, the cerebrum was divided into the following structures: cortical gray matter, subcortical white matter, thalamus, caudate, putamen,

pallidum and hippocampus. Total intracranial volume (TICV) was computed for each participant. Cortical thickness measures were derived by first identifying white matter voxels to establish the gray-white matter interface as the starting point for cortical segmentation. Subsequently, a deformable surface algorithm was applied to construct the pial surface with submillimeter precision [24]. Segmentation requires the use of a set of priors in the form of an atlas, which guides the identification of specific brain structures based on location, tissue type and local spatial configuration [25]. The output was visually reviewed and topological inaccuracies were manually corrected. In order to align sulcal and gyral characteristics across participants, each reconstructed brain was registered to a common spherical representation coordinate system [26]. Parcellation of specific cortical areas was based on the system developed by Desikan et al. [27], and allowed for calculation of the mean thickness for each area. Cortical thickness estimates were determined by averaging the shortest distance from each point on the gray-white matter boundary to the pial surface and the shortest distance from every point on the pial surface to the gray-white matter boundary [24]. FreeSurfer's segmentation and parcellation approach has been shown to be robust to intensity overlap between different cortical structures and comparable to manual labeling in accuracy [27-29]. We have extended that comparison by demonstrating the enhanced validity of utilizing a set of manually edited pediatric priors for developmental studies [20].

Cognitive and Behavioral Assessment

Cognition was measured at 36 months of age using the Bayley Scales of Infant Development-II (BSID-II) Mental Scale, which tests memory, problem solving, early number concepts, generalization and vocalizations [30]. A standard score, the Mental Development Index (MDI), was derived, with a mean of 100 and an SD of 16. Behavior was assessed at 36 months using the Child Behavior Checklist (CBCL) – Parent [31]. Summary scores reported here are T scores (standardized by age and sex) for externalizing, internalizing and total problems. The cut-off point for the normal range of these summary scores is a T score <60, with borderline scores ranging from 60 to 63 and clinical scores ≤64.

Laboratory measurement of attention was assessed using the Conners' Kiddie Continuous Performance Test version 5 (K-CPT™ V.5), a 7.5-min computerized task administered at 66 months [32]. Children were presented with a series of common pictures on a computer screen and asked to press the space bar in response to every picture shown except in response to the picture of the ball. Pictures were presented for 500 ms with an inter-stimulus interval (ISI) that varied between 1.5 and 3.0 s. For each ISI, 5 blocks consisting of 20 trials (pictures) per block were presented. Reaction times (RT) were recorded to the nearest millisecond. RT less than 100 ms were considered perseverations or anticipatory rather than true responses. K-CPT measures of attention used in this study included omissions, commissions, hit reaction time (HRT) and HRT by ISI. Omissions were defined as the number of pictures to which the child did not respond. Commissions were the number of times the child responded to the picture of the ball. Sustained attention (vigilance) was assessed using the measure of HRT by block. HRT was computed as the mean response time in milliseconds for all target responses for all 5 blocks of each ISI. HRT by ISI measured the

slope of change in RT over the two ISIs. HRT by block measured the change in RT across the 5 blocks of 20 trials per ISI. Logarithmic transformations of RT were used to calculate HRT and HRT by ISI. Values for all measures were then converted to T scores comparing the participant's score with an age- and gender-matched normative group that had a mean of 50 and an SD of 10. High HRT T scores reflect slow RT and may be one indicator of inattentiveness. High HRT by ISI T scores reflect slowing of RT as the ISI lengthens, and may suggest problems adjusting to changing tempo and task demands. High HRT by block scores indicate slowing of RT as the test progresses and may suggest difficulty with sustained attention.

Covariates

Age at time of MRI, gender, handedness and TICV were included as covariates due to their previously reported influence on brain morphology [33-35]. Handedness was assessed at the 66-month IDEAL study visit by asking the caregiver to indicate which hand the child uses to write or draw with: left, right, both, or don't know.

Statistical Analysis

PME effects on subcortical and cortical brain volumes and cortical thickness were tested by the general linear model with type III sum of squares, adjusting for PTE, prenatal marijuana exposure, age at time of scan, gender, handedness, pulse sequence, and TICV (for volumetric outcomes). A similar analysis was done for PTE effects on subcortical and cortical brain volumes and cortical thickness, adjusting for PME and the above covariates. SAS 9.1.3 Service Pack 3 (SAS Institute Inc., Cary, N.C., USA) was used for statistical analysis. Analysis of variance, χ^2 test or Fisher's exact test was used, as appropriate, to examine group differences in demographic characteristics. Morphometric data derived from FreeSurfer analyses in which the majority of values were greater than two standard deviations from the mean were considered outliers and were eliminated from further analysis. For subcortical morphometric analyses, volumes were highly correlated between the two hemispheres; therefore, the average of each subcortical structure was computed and used as the unit of statistical measure for subsequent analyses. From the full FreeSurfer data set a priori, regions of interest (ROI) were extracted for the general linear model analyses based on previous imaging studies of PME [12, 13], PTE [19, 36] and attention-deficit hyperactivity disorder (ADHD) [37-39]. We included ROI previously reported to be related to ADHD because of the hypothesized link between PME, PTE and the later development of ADHD or ADHD-related endophenotypes [10, 40, 41]. ROI for the subcortical volumetric analyses included subcortical white matter, thalamus, caudate, putamen, pallidum and hippocampus. ROI for the cortical volumetric and thickness analyses included TICV, cortical gray matter, the left and right dorsolateral prefrontal cortex (DLPFC), anterior cingulate gyrus, orbital-frontal cortex (OFC), posterior cingulate, inferior frontal gyrus, inferior parietal lobule, superior temporal gyrus, posterior aspect of the superior temporal sulcus (Banks) and the lingual gyrus. As per FreeSurfer convention, the DLPFC was further subdivided into the rostral and caudal middle frontal cortex [42]; the cingulate gyrus into the rostral and caudal anterior cingulate cortex; the OFC into the lateral and medial OFC; the inferior frontal gyrus into the pars opercularis, pars triangularis and pars orbitalis gyri, and the inferior parietal lobule into the inferior parietal cortex and the supramarginal gyrus.

Significance was defined as $p < 0.05$, but because of the small sample size and the exploratory nature of this study, we considered $p < 0.10$ as indicative of a trend towards significance. Linear regression (Pearson's r) was employed to evaluate the association between specific brain morphological measures and cognitive, behavioral and attentional outcome measures.

Results

Characteristics of the Sample

Demographic and clinical characteristics of the study cohort, stratified by PME and PTE, are presented in table 1. There were 20 participants with PME, 19 of whom also had concomitant PTE (95.0%). Of the 15 participants without PME, 7 had PTE (46.7%). Of the 26 participants with PTE, 19 had PME (73.1%), but only 1 (11.1%) of the 9 participants without PTE had PME. As expected from the original IDEAL study design, no differences were found by PME status in maternal education, insurance status or infant birth weight. PTE was unrelated to maternal education and insurance status, but was borderline significantly associated with reduced birth weight ($p = 0.064$). Additionally, we found no differences by either PME or PTE status in maternal age, prenatal care, Hollingshead ISP (a measure of SES) at birth, maternal depression or psychological distress over the first 3 years of the study, child gender, handedness or gestational age. PME and PTE were significantly coassociated ($p = 0.002$) and prenatal marijuana exposure was associated with PME ($p = 0.027$) but not PTE. PME was highly related to reduced head circumference ($p = 0.011$) at birth, but was not associated with either TICV ($p = 0.385$) or TICV after adjustment for age at time of MRI ($p = 0.336$; data not shown). Age at acquisition of MRI and number of participants scanned using the modified pulse sequence were unrelated to PME or PTE status. As illustrated in tables 2 and 3, the imaged participants were highly representative of both the overall and the nonimaged Hawaii-site IDEAL study cohorts, respectively, except for race and degree of PTE.

Child Neurodevelopmental Outcomes

The average age of administration of the neurodevelopmental tests was as follows: Bayley MDI: 37.06 ± 1.54 months; CBCL: 37.82 ± 2.99 months, and K-CPT: 68 ± 4.7 months. As shown in tables 2 and 3, there were no differences in Bayley MDI scores comparing imaged participants with the overall IDEAL study and the Hawaii site IDEAL study cohorts, and previously published research on the entire IDEAL cohort did not identify differences in 36-month Bayley MDI outcomes by PME status [43]. However, as shown in table 4, among the imaged cohort, significant group differences were found in 36-month Bayley MDI scores, with non-PME children showing poorer scores (PME: 89.56 ± 7.90 vs. non-PME: 81.14 ± 14.34; $p = 0.043$). This difference was largely attributable to one non-PME, non-PTE participant whose score of 49 was close to 2.5 SD below the mean for the non-PME group (PME: 89.56 ± 7.90 vs. non-PME: 83.62 ± 11.41; $p = 0.097$ for analysis without this participant). In contrast, PME was significantly associated with higher (worse) HRT by ISI scores (PME: 72.13 ± 20.41 vs. non-PME: 52.43 ± 7.54; $p = 0.002$) and borderline higher HRT by block scores (PME: 64.64 ± 26.86 vs. non-PME: 46.45 ± 24.41; $p = 0.060$). No

PME or PTE group differences were found in CBCL scores or in K-CPT omissions, commissions or overall HRT.

Imaging Data

Subcortical Volumes—Table 5 shows the relationship between PME and PTE on average volumes of cortical gray matter, subcortical white matter, thalamus, caudate, putamen, pallidum and hippocampus, adjusting for PTE (in the case of PME) or PME (in the case of PTE), marijuana, age at time of scan, gender, handedness, pulse sequence and total ICV. Also shown is the effect of PME and PTE on total ICV, adjusting for the same covariates except total ICV. Average caudate volumes were significantly reduced among children with PME (PME: 3,540.2 ± 272.6 vs. non-PME: 4,043.4 ± 326.5; p = 0.001), equivalent to an effect size of d = −1.67. No other group differences by PME or PTE were identified.

Regional Cortical Thickness—Regional cortical thickness analyses are shown in table 6. After adjustment for covariates, PME was borderline related to increased cortical thickness in the left hemisphere medial OFC (PME: 3.38 ± 0.29 vs. non-PME: 3.24 ± 0.25; p = 0.054), right lateral OFC (PME: 3.43 ± 0.35 vs. non-PME: 3.35 ± 0.19; p = 0.062), and right supramarginal gyrus (PME: 2.96 ± 0.39 vs. non-PME: 2.91 ± 0.37; p = 0.063).

In contrast, PTE was significantly related to cortical thinning in the right posterior aspect of the superior temporal sulcus (PTE: 2.93 ± 0.35 vs. non-PTE: 3.37 ± 0.32; p = 0.024) and the right lateral occipital cortex (PTE: 2.67 8 0.16 vs. non-PTE: 2.79 ± 0.20; p = 0.043), and borderline associated with cortical thinning in the caudal middle frontal region of the left DLPFC (PTE: 2.99 ± 0.20 vs. non-PTE: 3.10 ± 0.16; p = 0.058), the right supramarginal gyrus (PTE: 2.87 ± 0.38 vs. non-PTE: 3.13 ± 0.32; p = 0.082), the left superior temporal gyrus (PTE: 3.11 ± 0.24 vs. non-PTE: 3.30 ± 0.16; p = 0.069), the left lateral occipital cortex (PTE: 2.54 ± 0.18 vs. non-PTE: 2.70 ± 0.22; p = 0.074) and the left (PTE: 3.26 ± 0.29 vs. non-PTE: 3.58 ± 0.20; p = 0.095) and right (PTE: 3.17 ± 0.43 vs. non-PTE: 3.52 ± 0.23; p = 0.085) middle temporal gyri.

Regional Cortical Volumes—In general, there were few significant associations identified between PME or PTE and regional cortical volumes (table 7). After adjustment for covariates, PME was related to smaller volumes in the posterior aspect of the superior temporal sulcus (banks of superior temporal sulcus) on the right hemisphere (PME: 2,814.30 ± 593.83 vs. non-PME: 3,421.67 ± 745.28; p = 0.019) and borderline larger volumes in the right pars opercularis gyrus (PME: 4,958.40 ± 745.69 vs. non-PME: 4,486.07 ± 862.60; p = 0.074). PTE was associated with borderline smaller volumes in the right rostral anterior cingulate (PTE: 1,905.96 ± 355.77 vs. non-PTE: 2,048.67 ± 433.05; p = 0.054) and larger volumes in the left frontal pole (PTE: 1,033.54 ± 292.18 vs. non-PTE: 909.33 ± 218.62; p = 0.069).

Correlation Analyses—As shown in figure 1, there were highly significant correlations between PME, average caudate volume and K-CPT HRT by ISI scores, suggesting that caudate volume mediates the relationship between PME and K-CPT HRT by ISI. There was

no association between caudate volume and HRT by block ($r = -0.191$; $p = 0.295$). Caudate volume was inversely associated with Bayley MDI scores ($r = -0.357$; $p = 0.045$), but the directionality of this relationship was not affected by PME status (PME: $r = -0.235$; $p = 0.347$; non-PME: $r = -0.149$; $p = 0.610$). This association was largely attributable to one non-PME, non-PTE participant whose score of 49 was close to 2.5 SD below the mean for the non-PME group, and whose caudate volume was 4,170 mm^3, one of the larger volumes in our cohort ($r = -0.309$; $p = 0.091$, for analysis without this participant). Caudate volume was not associated with the behavioral outcomes measured. No other associations were found between any of the significant or borderline significant measures in subcortical volume or cortical ROIs (both volume and thickness) and cognitive, behavioral or attentional outcomes.

Discussion

Using multiple regression analysis with adjustment for important covariates, we identified significant volumetric reductions in the caudate nucleus among preschool-aged children with PME followed prospectively since birth. The magnitude of the volume reduction was large as measured by Cohen's d. We additionally found selected PME- and PTE-associated group differences in regional cortical volume and thickness measures, consistent with the postulated neurodevelopmental effects of MA and tobacco. Our findings refine and extend previously published research by: (1) examining a priori-defined ROIs among a cohort of preschool-aged children with prenatal drug exposure and an age- and socio-demographically matched comparison group followed prospectively since birth; (2) excluding children with prenatal alcohol exposure, and (3) using an analysis strategy designed to uncover the independent contributions of PME versus PTE on brain morphometry.

The large PME-associated volume reductions observed in the caudate region in this study are consistent with previous neuroimaging research [12, 13] and with a large body of clinical and basic science research on the neurotoxicity of MA to striatal neurons [44, 45]. Our findings of reduced caudate volumes parallel those seen in adolescents with prenatal cocaine exposure [46], another stimulant with pharmacologic properties like MA. The caudate volume deficits seen in our study (12.4%) were also of similar magnitude to the reductions attributed to PME in the Chang et al. [12] and Sowell et al. [13] studies, 13 and 10–15%, respectively, lending additional validity to our results. To test for evidence of a dose response on striatal neurotoxicity, we examined the relationship between the level of MA exposure [none, some (<3 days/week) and heavy (≥ 3 days/week)] and caudate volume. While the overall ANOVA was highly significant [$F(2, 31) = 11.27$, $p = 0.0002$], the only group difference that retained significance after Bonferroni multiple comparison test was between some exposure and no exposure (difference of means: −509.5; 95% CI: −787.0, −232.0; $p < 0.05$).

Sowell et al. [13] found that smaller caudate volumes in children with PME were associated with lower full-scale intelligence quotients (FSIQ), but paradoxically with higher FSIQ scores in children without PME. In their discussion, however, they suggest caution in interpreting their preliminary finding. In our study we found a significant inverse relationship between caudate volumes and Bayley MDI scores, a construct analogous to

FSIQ, when PME and non-PME groups were combined, but the relationship, although in the same direction, was no longer significant when stratified. As described in the results section, the inverse relationship was skewed by a single participant who appeared to be an outlier. In combination with the lack of any association between PME and Bayley MDI scores at 3 years of age in the entire IDEAL cohort [43], this suggests that the inverse relationship between caudate volumes and Bayley MDI scores found in our study was spurious. Consistent with this, several recent neuroimaging studies also did not find associations between caudate volumes and FSIQ or Bayley MDI scores [47, 48].

Cumulative evidence suggests that, rather than directly determining intelligence, the caudate functions instead in cognitive control processes such as the flexibility of responding and the ability to change or regulate behaviors when task contingencies or goals change [49, 50]. Our findings relating PME, caudate volume and HRT by ISI scores, the latter possibly indicating a difficulty adjusting to changing task demands, provide support for this caudate-cognitive control relationship, and suggest a more subtle alteration in the neurodevelopment of children with PME. Additionally, our findings relating PME to worse K-CPT HRT by block scores, suggesting difficulty with sustained attention, replicate previous research [12] in which PME was related to poorer performance on another sustained attention task, the Test of Variable Attention [51]. Of note, we did not find accompanying group differences in omissions or commissions, nor did we find brain behavior correlations with the HRT by block scores. Similar subtle deficits in attentional functioning as were seen in participants in this neuroimaging study have been recently confirmed in the entire IDEAL cohort among children with PME [52].

Our PME- and PTE-associated cortical thickness findings showed regional coherence with the existing literature and hypothesized PME and PTE effects. For example, we found borderline increased cortical thickness in the left medial OFC, right lateral OFC and the right supramarginal gyrus, part of the right inferior parietal lobule, consistent with prior research implicating these regions with both stimulant exposure and attention [38, 53, 54]. Although these thickness increases have not been previously described in the literature on PME, they have been observed in children with prenatal alcohol exposure [55], where they were thought to reflect either compensatory or aberrant CNS development. If confirmed in larger samples, these thickness increases may be consistent with the PME-associated cortical volumetric increases described by Sowell et al. [13]. We additionally found possible PTE-associated cortical thinning in several cortical regions implicated in previous neuroimaging studies of PTE, including the caudal middle frontal and the temporal lobe [19, 36], the latter consistent with the known effects of PTE on auditory processing [56]. If confirmed in studies with greater power, our results suggest that prenatal MA and prenatal tobacco may have distinct differential cortical effects on the developing CNS.

Overall, we found little evidence for widespread cortical volumetric or thickness changes among preschool-aged children as a result of PME or PTE, although our relatively small sample size may have limited our ability to identify group differences. Nevertheless, the regions where we did see borderline and significant differences were consistent with areas identified in previous studies and with the hypothesized effects of MA and tobacco on the developing CNS [40]. For example, the borderline PME-associated volumetric increases

seen in the right pars opercularis are consistent with the perisylvian cortex volumetric increases identified by Sowell et al. [13], but we also found PME-associated volume deficits in the right posterior aspect of the superior temporal sulcus. The borderline volume reductions seen here in the right rostral anterior cingulate associated with PTE were in contrast to those seen by Sowell et al. [13], who found PME-associated volume increases. Their study did not control for or measure PTE, so it is possible that doing so might have altered their results, a limitation acknowledged in their discussion. Given that several studies have described cingulate cortex volumetric reductions in children [57] and adults [58] with ADHD, along with the well-known association between PTE and ADHD [59] and the recently described one between PME and increased CBCL externalizing and ADHD problem behaviors in 5-year-old children [10], both our findings and those of Sowell et al. [13] show consistent regional specificity.

There are several limitations to this study, the major one being the relatively small sample sizes of the exposed and unexposed groups, which may have reduced our power to detect significant differences or, conversely, have inflated our results. In fact, after adjusting our subcortical and cortical results for multiple comparisons using the step-up Hochberg Bonferroni method [60], only the caudate volume reduction remained significant at the $p < 0.05$ level, although the volume reduction and cortical thinning seen in the posterior aspect of the right superior temporal sulcus indicated a trend toward significance with a $p < 0.1$. Therefore, we would consider all of the results herein to be preliminary with the exception of the findings on reduced caudate volumes associated with PME. A second potential limitation comes from trying to separately adjust for PME and PTE in our analyses, given the very high degree of correlation between the two exposures as shown in table 1. Disentangling the effects of individual drugs among pregnant women who are poly-substance users is a challenge [61]. As such, it is possible that residual confounding may alternatively explain the observed findings. Third, our ability to identify group differences may have been minimized because of offsetting effects of PME and PTE among participants with coexposure (19 out of 35 participants), as PME tended to make the cortex thicker, while PTE tended to make the cortex thinner. Fourth, although this study has definite methodological strengths over studies derived from community convenience samples, it is still possible that there was selection bias in recruitment, in that caregivers with children having developmental delays or behavioral concerns may have been more inclined to enroll. Finally, because this was a cross-sectional study, differentiation of actual causal processes from epiphenomena and compensatory responses is difficult [62].

Conclusion

Consistent with previous research, we found significant volume reductions in subcortical striatal structures related to PME. Reduced caudate volume appears to mediate the relationship found between PME and K-CPT reaction time by ISI outcomes, a subtle EF deficit suggesting that exposed children may have more difficulty adjusting to changing task demands. We also identified PME-associated cortical thickness increases in perisylvian and orbital-frontal cortices, a finding similar to the volumetric increases described by Sowell [13]. In contrast to PME, PTE appears to be associated with cortical thinning in perisylvian

and lateral occipital cortices, and with possible volumetric increases in frontal and volumetric decreases in anterior cingulate regions.

Acknowledgments

This study was sbupported by K23DA020801 (C.D.), R01DA017905 and K02DA000354 (B.K.), R01DA014948 (B.L.) and U54RR026136/U54MD007584 (Hedges JR, Dean of the University of Hawaii School of Medicine). We would like to thank JoAnn Cheung, MA, Loree Shiroma and Kili Fern for their efforts in data collection and family support, and Lynne Dansereau, MSPH, for her assistance in providing IDEAL study data. Special thanks to all of the children and caregivers who participated.

References

1. Arria A, Derauf C, LaGasse L, Grant P, Shah R, Smith L, Haning W, Huestis M, Strauss A, Della Grotta S, Liu J, Lester B. Methamphetamine and other substance use during pregnancy: preliminary estimates from the Infant Development, Environment, and Lifestyle (IDEAL) Study. Matern Child Health J. 2006; 10:293–302. [PubMed: 16395620]
2. Thompson BL, Levitt P, Stanwood GD. Prenatal exposure to drugs: effects on brain development and implications for policy and education. Nat Rev Neurosci. 2009; 10:303–312. [PubMed: 19277053]
3. Salisbury AL, Ponder KL, Padbury JF, Lester BM. Fetal effects of psychoactive drugs. Clin Perinatol. 2009; 36:595–619. [PubMed: 19732616]
4. Frost DO, Cadet JL. Effects of methamphetamine-induced neurotoxicity on the development of neural circuitry: a hypothesis. Brain Res Brain Res Rev. 2000; 34:103–118. [PubMed: 11113502]
5. Lester BM, Padbury JF. Third pathophysiology of prenatal cocaine exposure. Dev Neurosci. 2009; 31:23–35. [PubMed: 19372684]
6. Tata DA, Yamamoto BK. Interactions between methamphetamine and environmental stress: role of oxidative stress, glutamate and mitochondrial dysfunction. Addiction. 2007; 102(suppl 1):49–60. [PubMed: 17493053]
7. Nguyen D, Smith LM, Lagasse LL, Derauf C, Grant P, Shah R, Arria A, Huestis MA, Haning W, Strauss A, Della Grotta S, Liu J, Lester BM. Intrauterine growth of infants exposed to prenatal methamphetamine: results from the infant development, environment, and lifestyle study. J Pediatr. 2010; 157:337–339. [PubMed: 20570284]
8. Lagasse LL, Wouldes T, Newman E, Smith LM, Shah RZ, Derauf C, Huestis MA, Arria AM, Grotta SD, Wilcox T, Lester BM. Prenatal methamphetamine exposure and neonatal neurobehavioral outcome in the USA and New Zealand. Neurotoxicol Teratol. 2011; 33:166–175. [PubMed: 20615464]
9. Smith LM, LaGasse L, Derauf C, Grant P, Shah R, Arria A, Huestis M, Haning W, Strauss A, Della Grotta S, Fallone M, Liu J, Lester BM. Prenatal methamphetamine use and neonatal neurobehavioral outcome. Neurotoxicol Teratol. 2008; 30:20–28. [PubMed: 18031987]
10. LaGasse LL, Derauf C, Smith LM, Newman E, Shah R, Neal C, Arria A, Huestis MA, Della Grotta S, Lin H, Dansereau LM, Lester BM. Prenatal methamphetamine exposure and childhood behavior problems at ages 3 and 5. Pediatrics. 2012; 129:681–688. [PubMed: 22430455]
11. Derauf C, LaGasse LL, Smith LM, Newman E, Shah R, Neal C, Arria A, Huestis MA, Della Grotta S, Dansereau LM, Lin H, Lester BM. Prenatal methamphetamine exposure and inhibitory control among young school-age children. J Pediatr. 2012 E-pub ahead of print.
12. Chang L, Smith LM, LoPresti C, Yonekura ML, Kuo J, Walot I, Ernst T. Smaller subcortical volumes and cognitive deficits in children with prenatal methamphetamine exposure. Psychiatry Res. 2004; 132:95–106. [PubMed: 15598544]
13. Sowell ER, Leow AD, Bookheimer SY, Smith LM, O'Connor MJ, Kan E, Rosso C, Houston S, Dinov ID, Thompson PM. Differentiating prenatal exposure to methamphetamine and alcohol versus alcohol and not methamphetamine using tensor-based brain morphometry and discriminant analysis. J Neurosci. 2010; 30:3876–3885. [PubMed: 20237258]

14. Frank DA, Augustyn M, Knight WG, Pell T, Zuckerman B. Growth, development, and behavior in early childhood following prenatal cocaine exposure: a systematic review. JAMA. 2001; 285:1613–1625. [PubMed: 11268270]
15. Bauer CR, Langer JC, Shankaran S, Bada HS, Lester B, Wright LL, Krause-Steinrauf H, Smeriglio VL, Finnegan LP, Maza PL, Verter J. Acute neonatal effects of cocaine exposure during pregnancy. Arch Pediatr Adolesc Med. 2005; 159:824–834. [PubMed: 16143741]
16. Norman AL, Crocker N, Mattson SN, Riley EP. Neuroimaging and fetal alcohol spectrum disorders. Dev Disabil Res Rev. 2009; 15:209–217. [PubMed: 19731391]
17. Zhou D, Lebel C, Lepage C, Rasmussen C, Evans A, Wyper K, Pei J, Andrew G, Massey A, Massey D, Beaulieu C. Developmental cortical thinning in fetal alcohol spectrum disorders. Neuroimage. 2011; 58:16–25. [PubMed: 21704711]
18. Yang Y, Roussotte F, Kan E, Sulik KK, Mattson SN, Riley EP, Jones KL, Adnams CM, May PA, O'Connor MJ, Narr KL, Sowell ER. Abnormal cortical thickness alterations in fetal alcohol spectrum disorders and their relationships with facial dysmorphology. Cereb Cortex 2011. 2012; 22:1170–1179.
19. Toro R, Leonard G, Lerner JV, Lerner RM, Perron M, Pike GB, Richer L, Veillette S, Pausova Z, Paus T. Prenatal exposure to maternal cigarette smoking and the adolescent cerebral cortex. Neuropsychopharmacology. 2008; 33:1019–1027. [PubMed: 17609681]
20. Quinn, B.; Shienkopf, S.; Kennedy, D.; Fischl, B.; Kosofsky, B. Assessment of validity of probabilistic atlases for automated subcortical brain structures in pediatric population (abstract No. 464). Neuroimage; Abstracts of the 12th Annual Meeting of the Organization for Human Brain Mapping; 2006. p. e1
21. Smith LM, LaGasse LL, Derauf C, Grant P, Shah R, Arria A, Huestis M, Haning W, Strauss A, Della Grotta S, Liu J, Lester BM. The infant development, environment, and lifestyle study: effects of prenatal methamphetamine exposure, polydrug exposure, and poverty on intrauterine growth. Pediatrics. 2006; 118:1149–1156. [PubMed: 16951010]
22. Dale AM, Fischl B, Sereno MI. Cortical surface-based analysis. I. Segmentation and surface reconstruction. Neuroimage. 1999; 9:179–194. [PubMed: 9931268]
23. Fischl B, Sereno MI, Tootell RB, Dale AM. High-resolution intersubject averaging and a coordinate system for the cortical surface. Hum Brain Map. 1999; 8:272–284.
24. Fischl B, Dale AM. Measuring the thickness of the human cerebral cortex from magnetic resonance images. Proc Natl Acad Sci USA. 2000; 97:11050–11055. [PubMed: 10984517]
25. Walhovd KB, Fjell AM, Reinvang I, Lundervold A, Dale AM, Eilertsen DE, Quinn BT, Salat D, Makris N, Fischl B. Effects of age on volumes of cortex, white matter and subcortical structures. Neurobiol Aging. 2005; 26:1261–1270. [PubMed: 16005549]
26. Fischl B, Liu A, Dale AM. Automated manifold surgery: constructing geometrically accurate and topologically correct models of the human cerebral cortex. IEEE Trans Med Imaging. 2001; 20:70–80. [PubMed: 11293693]
27. Desikan RS, Ségonne F, Fischl B, Quinn BT, Dickerson BC, Blacker D, Buckner RL, Dale AM, Maguire RP, Hyman BT, Albert MS, Killiany RJ. An automated labeling system for subdividing the human cerebral cortex on MRI scans into gyral based regions of interest. Neuroimage. 2006; 31:968–980. [PubMed: 16530430]
28. Fischl B, Salat DH, Busa E, Albert M, Dieterich M, Haselgrove C, van der Kouwe A, Killiany R, Kennedy D, Klaveness S, Montillo A, Makris N, Rosen B, Dale AM. Whole brain segmentation: automated labeling of neuroanatomical structures in the human brain. Neuron. 2002; 33:341–355. [PubMed: 11832223]
29. Fjell AM, Walhovd KB, Reinvang I, Lundervold A, Dale AM, Quinn BT, Makris N, Fischl B. Age does not increase rate of forgetting over weeks – neuro anatomical volumes and visual memory across the adult lifespan. J Int Neuropsychol Soc. 2005; 11:2–15. [PubMed: 15686603]
30. Bayley, N. Bayley Scales of Infant Development. 2. New York: Psychological Corporation; 1993.
31. Achenbach, TM.; Rescorla, LA. Manual for the ASEBA Preschool Forms and Profiles. Burlington: University of Vermont, Research Center for Children, Youth, and Families; 2000.

32. Conners, C., editor. Conners' Kiddie Continuous Performance Test (K-CPT ™): Version 5 for Windows® – Technical Guide and Software Manual. North Tonawanda: Multi-Health Systems; 2006.
33. Good CD, Johnsrude IS, Ashburner J, Henson RN, Friston KJ, Frackowiak RS. Cerebral asymmetry and the effects of sex and handedness on brain structure: a voxel-based morphometric analysis of 465 normal adult human brains. Neuroimage. 2001; 14:685–700. [PubMed: 11506541]
34. Rivkin MJ, Davis PE, Lemaster JL, Cabral HJ, Warfield SK, Mulkern RV, Robson CD, Rose-Jacobs R, Frank DA. Volumetric MRI study of brain in children with intrauterine exposure to cocaine, alcohol, tobacco, and marijuana. Pediatrics. 2008; 121:741–50. [PubMed: 18381539]
35. Gallinat J, Meisenzahl E, Jacobsen LK, Kalus P, Bierbrauer J, Kienast T, Witthaus H, Leopold K, Seifert F, Schubert F, Staedtgen M. Smoking and structural brain deficits: a volumetric MR investigation. Eur J Neurosci. 2006; 24:1744–1750. [PubMed: 17004938]
36. Jacobsen LK, Slotkin TA, Mencl WE, Frost SJ, Pugh KR. Gender-specific effects of prenatal and adolescent exposure to tobacco smoke on auditory and visual attention. Neuropsychopharmacology. 2007; 32:2453–2464. [PubMed: 17375135]
37. Batty MJ, Liddle EB, Pitiot A, Toro R, Groom MJ, Scerif G, Liotti M, Liddle PF, Paus T, Hollis C. Cortical gray matter in attention-deficit/hyperactivity disorder: a structural magnetic resonance imaging study. J Am Acad Child Adolesc Psychiatry. 2010; 49:229–238. [PubMed: 20410712]
38. Makris N, Biederman J, Valera EM, Bush G, Kaiser J, Kennedy DN, Caviness VS, Faraone SV, Seidman LJ. Cortical thinning of the attention and executive function networks in adults with attention-deficit/hyperactivity disorder. Cereb Cortex. 2007; 17:1364–1375. [PubMed: 16920883]
39. Casey BJ, Epstein JN, Buhle J, Liston C, Davidson MC, Tonev ST, Spicer J, Niogi S, Millner AJ, Reiss A, Garrett A, Hinshaw SP, Greenhill LL, Shafritz KM, Vitolo A, Kotler LA, Jarrett MA, Glover G. Frontostriatal connectivity and its role in cognitive control in parent-child dyads with ADHD. Am J Psychiatry. 2007; 164:1729–1736. [PubMed: 17974939]
40. Derauf C, Kekatpure M, Neyzi N, Lester B, Kosofsky B. Neuroimaging of children following prenatal drug exposure. Semin Cell Dev Biol. 2009; 20:441–454. [PubMed: 19560049]
41. Froehlich TE, Lanphear BP, Auinger P, Hornung R, Epstein JN, Braun J, Kahn RS. Association of tobacco and lead exposures with attention-deficit/hyperactivity disorder. Pediatrics. 2009; 124:e1054–e1063. [PubMed: 19933729]
42. Kikinis Z, Fallon JH, Niznikiewicz M, Nestor P, Davidson C, Bobrow L, Pelavin PE, Fischl B, Yendiki A, McCarley RW, Kikinis R, Kubicki M, Shenton ME. Gray matter volume reduction in rostral middle frontal gyrus in patients with chronic schizophrenia. Schizophr Res. 2010; 123:153–159. [PubMed: 20822884]
43. Smith LM, LaGasse LL, Derauf C, Newman E, Shaw R, Haning W, Arria A, Huestis M, Strauss A, Della Grotta S, Dansereau LM, Lin H, Lester BM. Motor and cognitive outcomes through three years of age in children exposed to prenatal methamphetamine. Neurotox Teratol. 2011; 33:176–184.
44. Yamamoto BK, Moszczynska A, Gudelsky GA. Amphetamine toxicities. Ann NY Acad Sci. 2010; 1187:101–121. [PubMed: 20201848]
45. Zhu JPQ, Xu W, Angulo JA. Methamphetamine-induced cell death: selective vulnerability in neuronal subpopulations of the striatum in mice. Neuroscience. 2006; 140:607–622. [PubMed: 16650608]
46. Avants BB, Hurt H, Giannetta JM, Epstein CL, Shera DM, Rao H, Wang J, Gee JC. Effects of heavy in utero cocaine exposure on adolescent caudate morphology. Pediatr Neurol. 2007; 37:275–279. [PubMed: 17903672]
47. Peterson BS, Vohr B, Staib LH, Cannistraci CJ, Dolberg A, Schneider KC, Katz KH, Westerveld M, Sparrow S, Anderson AW, Duncan CC, Makuch RW, Gore JC, Ment LR. Regional brain volume abnormalities and long-term cognitive outcome in preterm infants. JAMA. 2000; 284:1939–1947. [PubMed: 11035890]
48. Peterson BS, Anderson AW, Ehrenkranz R, Staib LH, Tageldin M, Colson E, Gore JC, Duncan CC, Makuch R, Ment LR. Regional brain volumes and their later neurodevelopmental correlates in term and preterm infants. Pediatrics. 2003; 111:939–948. [PubMed: 12728069]

49. Grahn JA, Parkinson JA, Owen AM. The cognitive functions of the caudate nucleus. Prog Neurobiol. 2008; 86:141–155. [PubMed: 18824075]
50. Casey BJ, Tottenham N, Fossella J. Clinical, imaging, lesion, and genetic approaches toward a model of cognitive control. Dev Psychobiol. 2002; 40:237–254. [PubMed: 11891636]
51. Greenberg LM. Test of variables of attention. J Clin Psychol. 1998; 54:461–476. [PubMed: 9623751]
52. Kiblawi, ZN.; Smith, LM.; LaGasse, LL.; Derauf, C.; Newman, E.; Shah, R.; Arria, A.; Huestis, MA.; DellaGrotta, S.; Dansereau, LM.; Neal, C.; Lester, BM. The effects of prenatal methamphetamine exposure on attention as assessed by continuous performance tests: results from the Infant, Development, Environment, and Lifestyle (IDEAL) Study. Abstract accepted for poster presentation at 2012 Pediatric Academic Societies meeting;
53. Raz A, Buhle J. Typologies of attentional networks. Nat Rev Neurosci. 2006; 7:367–379. [PubMed: 16760917]
54. Sowell ER, Thompson PM, Welcome SE, Henkenius AL, Toga AW, Peterson BS. Cortical abnormalities in children and adolescents with attention-deficit hyperactivity disorder. Lancet. 2003; 362:1699–1707. [PubMed: 14643117]
55. Sowell ER, Mattson SN, Kan E, Thompson PM, Riley EP, Toga AW. Abnormal cortical thickness and brain-behavior correlation patterns in individuals with heavy prenatal alcohol exposure. Cereb Cortex. 2008; 18:136–144. [PubMed: 17443018]
56. Fried PA, Watkinson B, Gray R. Differential effects on cognitive functioning in 13- to 16-year-olds prenatally exposed to cigarettes and marijuana. Neurotoxicol Teratol. 2003; 25:427–436. [PubMed: 12798960]
57. Overmeyer S, Bullmore ET, Suckling J, Simmons A, Williams SC, Santosh PJ, Taylor E. Distributed grey and white matter deficits in hyperkinetic disorder: MRI evidence for anatomical abnormality in an attentional network. Psychol Med. 2001; 31:1425–1435. [PubMed: 11722157]
58. Seidman LJ, Valera EM, Makris N, Monuteaux MC, Boriel DL, Kelkar K, Kennedy DN, Caviness VS, Bush G, Aleardi M, Faraone SV, Biederman J. Dorsolateral prefrontal and anterior cingulated cortex volumetric abnormalities in adults with attention-deficit/hyperactivity disorder identified by magnetic resonance imaging. Biol Psychiatry. 2006; 60:1071–1080. [PubMed: 16876137]
59. Cornelius MD, Day NL. Developmental consequences of prenatal tobacco exposure. Curr Opin Neurol. 2009; 22:121–125. [PubMed: 19532034]
60. Hochberg Y. A sharper Bonferroni procedure for multiple tests of significance. Biometrika. 1988; 75:800–802.
61. Lebel C, Sowell E. Diffusion tensor imaging studies of prenatal drug exposure: challenges of poly-drug use in pregnant women. J Pediatr. 2011; 159:709–710. [PubMed: 21813134]
62. Peterson BS. Conceptual, methodological, and statistical challenges in brain imaging studies of developmentally based psychopathologies. Dev Psychopathol. 2003; 15:811–832. [PubMed: 14582941]

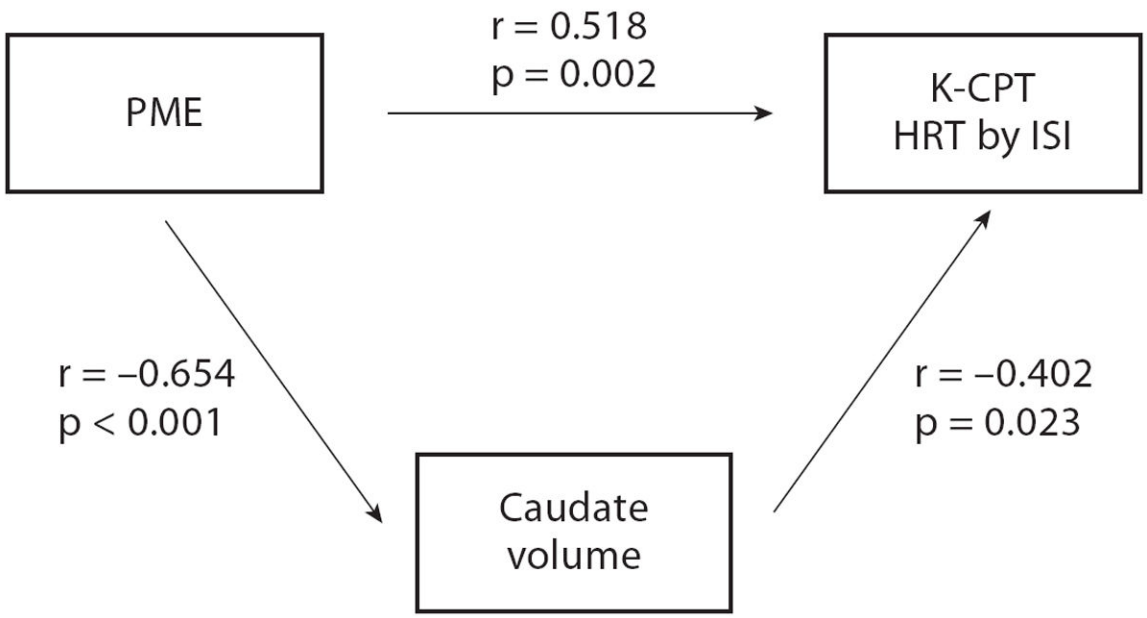

Fig. 1.
Correlations between PME, average caudate volume and K-CPT HRT by ISI.

Table 1

Sociodemographic, clinical and MRI characteristics of imaged participants

	PME			PTE		
	non-PME (n = 15)	**PME (n = 20)**	**p**	**non-PTE (n = 9)**	**PTE (n = 26)**	**p**
Maternal variables						
Education (<high school)	8 (53.3%)	10 (50.0%)	0.850	3 (33.3%)	15 (57.7%)	0.264
Age, years	22.3 (3.0)	25.5 (6.7)	0.096	23.9 (6.2)	24.2 (5.5)	0.905
Public insurance (yes)	13 (86.7%)	17 (85.0%)	0.889	8 (88.9%)	22 (84.6%)	0.752
Gestational age at first prenatal visit, weeks	9.4 (4.8)	12.1 (4.6)	0.139	9.5 (4.5)	11.4 (4.9)	0.357
Hollingshead ISP (birth)	25.60 (7.56)	23.45 (9.26)	0.468	28.39 (7.21)	22.98 (8.62)	0.102
Hollingshead ISP (average)	27.33 (5.77)	29.52 (8.01)	0.377	30.01 (6.33)	28.08 (7.43)	0.493
PTE (yes)	7 (46.7%)	19 (95.0%)	0.002	–	–	–
PME (yes)	–	–	–	1 (11.1%)	19 (73.1%)	0.002
Prenatal marijuana (yes)	0	6 (30.0%)	0.027	0	6 (23.1%)	0.304
Depression (BDI average)	8.76 (6.45)	6.81 (7.46)	0.425	9.74 (7.11)	6.92 (6.97)	0.305
Psychological distress (BSI average)	0.43 (0.37)	0.36 (0.43)	0.640	0.49 (0.44)	0.36 (0.39)	0.420
Child variables						
Gender (male)	8 (53.3%)	11 (55.0%)	0.925	3 (33.3%)	16 (61.5%)	0.245
Handedness (right)[1]	12 (85.7%)	16 (80%)	1.000	9 (100%)	19 (76%)	0.162
Birth weight, g	3,276.47 (641.31)	3,139.75 (581.39)	0.515	3,517.56 (446.86)	3,087.85 (616.71)	0.064
Birth head circumference, cm	34.53 (1.60)	33.05 (1.61)	0.011	34.44 (1.01)	33.42 (1.88)	0.132
Gestational age, weeks	39.20 (1.15)	38.55 (1.85)	0.240	39.56 (1.24)	38.58 (1.65)	0.115
Imaging variables						
MRI age, months	47.26 (7.88)	45.76 (6.78)	0.547	46.33 (8.59)	46.43 (6.85)	0.972
Modified MPRage pulse sequence	3 (20.0%)	3 (15.0%)	1.000	3 (33.3%)	3 (11.5%)	0.162

Values are mean with SD in parentheses or number with percentage in parentheses. Means computed using ANOVA. Frequencies computed by χ^2 or by Fisher's exact test (two-sided).

[1] One participant with no handedness data.

Table 2

Comparison of Hawaii IDEAL MR-imaged versus nonimaged multi-site IDEAL participants

	MR-imaged participants (n = 35)	Nonimaged IDEAL participants (n = 377)	p
Maternal/demographic characteristics			
Race			<0.001
White	4 (11.4%)	156 (41.4%)	
Hispanic	1 (2.9%)	91 (24.1%)	
Hawaiian/Pacific Islander	20 (57.1%)	51 (13.5%)	
Asian	7 (20.0%)	50 (13.3%)	
Black	3 (8.6%)	18 (4.8%)	
American Indian	0	10 (2.7%)	
Other	0	1 (0.3%)	
Low SES (Hollingshead V)	11 (31.4%)	82 (21.9%)	0.196
Public insurance	30 (85.7%)	333 (88.3%)	0.648
Partner at birth	17 (48.6%)	210 (55.7%)	0.417
Education <12 years	18 (51.4%)	154 (41.1%)	0.235
Maternal age, years	24.1 (5.6)	25.3 (5.6)	0.232
Gestational age at first prenatal visit, weeks	10.9 (4.8)	12.1 (7.5)	0.398
Prenatal MA use	20 (57.1%)	184 (48.8%)	0.345
Heavy MA use (≥3 days/week across pregnancy)	3 (8.8%)	32 (8.6%)	0.645
Prenatal tobacco use	26 (74.3%)	192 (50.9%)	0.008
Prenatal marijuana use	6 (17.1%)	70 (18.6%)	0.835
Neonatal/child characteristics			
Gender (boy)	19 (54.3%)	201 (53.3%)	0.912
Birth weight, g	3,198 (602)	3,252 (599)	0.612
Length, cm	50.5 (3.0)	50.4 (3.4)	0.831
Head circumference, cm	33.7 (1.7)	33.9 (1.8)	0.515
Gestational age, weeks	38.8 (1.6)	38.6 (2.1)	0.593
SGA	8 (22.9%)	47 (12.5%)	0.084
Low birth weight (<2,500 g)	3 (8.6%)	44 (11.7%)	0.581
BSID-II MDI[1]	85.9 (11.8)	88.6 (13.6)	0.273

Values are number with percentage in parentheses or mean with SD in parentheses. SGA = Small for gestational age.

[1] Measured at the 3-year visit: 32 MRI participants, 244 remaining IDEAL participants.

Table 3

Comparison of MR-imaged versus nonimaged Hawaii-site IDEAL participants

	MR-imaged participants (n = 35)	Nonimaged Hawaii IDEAL participants (n = 124)	p
Maternal/demographic characteristics			
Race			0.106
White	4 (11.4%)	22 (17.7%)	
Hispanic	1 (2.9%)	12 (9.7%)	
Hawaiian/Pacific Islander	20 (57.1%)	45 (36.3%)	
Asian	7 (20.0%)	40 (32.3%)	
Black	3 (8.6%)	5 (4.0%)	
Low SES (Hollingshead V)	11 (31.4%)	36 (29.0%)	0.784
Public insurance	30 (85.7%)	109 (87.9%)	0.730
Partner at birth	17 (48.6%)	72 (58.1%)	0.318
Education <12 years	18 (51.4%)	52 (41.9%)	0.318
Maternal age, years	24.1 (5.6)	25.0 (5.4)	0.368
Gestational age at first prenatal visit, weeks	10.9 (4.8)	13.0 (7.5)	0.141
Prenatal MA use	20 (57.1%)	60 (48.4%)	0.360
Heavy MA use (≥3 days/week across pregnancy)	3 (8.8%)	14 (11.7%)	0.437
Prenatal tobacco use	26 (74.3%)	69 (55.6%)	0.047
Prenatal marijuana use	6 (17.1%)	15 (12.1%)	0.436
Neonatal/child characteristics			
Gender (boy)	19 (54.3%)	64 (51.6%)	0.780
Birth weight, g	3,198 (602)	3,185 (518)	0.899
Length, cm	50.5 (3.0)	50.5 (2.7)	0.985
Head circumference, cm	33.7 (1.7)	33.8 (1.7)	0.731
Gestational age, weeks	38.8 (1.6)	38.5 (1.7)	0.370
SGA	8 (22.9%)	17 (13.7%)	0.189
Low birth weight (<2,500 g)	3 (8.6%)	12 (9.7%)	0.843
BSID-II MDI[1]	85.9 (11.8)	86.1 (17.1)	0.954

Values are number with percentage in parentheses or mean with SD in parentheses. SGA = Small for gestational age.

[1] Measured at the 3-year visit: 32 MR-imaged participants, 74 nonimaged Hawaii IDEAL participants.

Table 4

Cognitive, behavioral and attentional outcomes of imaged participants

	PME			PTE		
	non-PME (n = 15)	**PME (n = 20)**	**p**	**non-PTE (n = 9)**	**PTE (n = 26)**	**p**
Bayley MDI	81.14 (14.34)	89.56 (7.90)	0.043	80.25 (17.14)	87.75 (9.08)	0.120
CBCL externalizing	60.47 (11.18)	58.85 (15.27)	0.732	60.78 (13.57)	59.12 (13.72)	0.756
CBCL internalizing	50.53 (9.08)	54.10 (11.35)	0.325	52.78 (12.26)	52.50 (10.01)	0.946
CBCL total	56.33 (8.97)	57.40 (11.66)	0.770	57.11 (13.64)	56.88 (9.45)	0.956
K-CPT omissions	69.42 (33.57)	73.34 (28.34)	0.731	63.12 (27.92)	75.29 (31.08)	0.321
K-CPT commissions	60.30 (13.84)	56.03 (10.69)	0.348	60.08 (12.76)	56.94 (12.03)	0.525
K-CPT hit RT	46.47 (13.38)	50.92 (14.43)	0.396	49.53 (12.99)	48.76 (14.62)	0.891
K-CPT hit RT by block	46.45 (24.41)	64.64 (26.86)	0.060	49.61 (21.79)	60.24 (28.73)	0.326
K-CPT hit RT by ISI	52.43 (7.54)	72.13 (20.41)	0.002	56.14 (8.05)	67.25 (21.16)	0.139

Values are mean with SD in parentheses.

Table 5

Average cortical and subcortical volumes of imaged participants in mm^3

	PME				PTE			
	non-PME (n = 15)	PME (n = 20)	t value	p[1]	non-PTE (n = 9)	PTE (n = 26)	t value	p[1]
Total ICV	1,446,001.6 (195,655.4)	1,388,466.8 (188,009.6)	–1.31	0.200	1,423,375.4 (206,228.0)	1,409,576.2 (189,145.4)	–0.58	0.569
Cortical gray	325,318.5 (14,297.8)	312,931.3 (28,508.0)	–0.57	0.574	329,127.4 (14,613.6)	314,471.4 (25,670.3)	–1.30	0.205
Subcortical white	180,767.7 (31,037.5)	170,527.2 (25,064.7)	–1.82	0.080	167,702.6 (20,155.7)	177,412.9 (29,961.1)	0.50	0.623
Thalamus	6,515.2 (668.8)	6,360.1 (536.6)	–1.40	0.172	6,371.4 (478.6)	6,445.7 (634.7)	–0.06	0.950
Caudate	4,043.4 (326.5)	3,540.2 (272.6)	–3.67	0.001*	3,961.8 (244.0)	3,684.6 (404.3)	0.07	0.942
Putamen	5,151.1 (350.9)	4,998.4 (482.3)	–0.42	0.675	5,104.5 (367.1)	5,049.8 (458.1)	–0.15	0.881
Pallidum	1,295.2 (127.2)	1,254.8 (146.0)	–0.75	0.459	1,284.9 (131.6)	1,267.6 (142.1)	–0.43	0.672
Hippocampus	3,874.6 (386.7)	3,772.6 (329.1)	–0.89	0.380	3,908.4 (202.5)	3,784.4 (390.4)	–0.70	0.491

Values in parentheses are SD. Volumes in each case are averaged across left and right hemispheres. No main effect of hemisphere for any structure.

[1] Adjusted for prenatal MA (or TOB), marijuana, age at time of scan, gender, handedness, pulse sequence and total intracranial volume.

* $p < 0.05$ after multiplicity adjustment within domain category using the step-up Hochberg Bonferroni method [60].

Table 6

Average cortical thickness of imaged participants in mm

Region	PME				PTE			
	non-PME (n = 15)	PME (n = 20)	t value	p[1]	non-PTE (n = 9)	PTE (n = 26)	t value	p[1]
DLPFC – left	3.06 (0.18)	3.00 (0.24)	–0.16	0.876	3.07 (0.22)	3.01 (0.22)	–0.56	0.580
Rostral middle frontal – left	3.07 (0.23)	3.00 (0.27)	–0.64	0.528	3.05 (0.26)	3.02 (0.26)	–0.05	0.959
Caudal middle frontal – left	3.02 (0.18)	3.01 (0.21)	1.44	0.162	3.10 (0.16)	2.99 (0.20)	–1.99	0.058
DLPFC – right	2.94 (0.22)	2.96 (0.29)	1.05	0.305	2.99 (0.28)	2.94 (0.26)	–0.71	0.484
Rostral middle frontal – right	2.93 (0.24)	2.94 (0.31)	0.95	0.352	2.97 (0.30)	2.93 (0.28)	–0.67	0.508
Caudal middle frontal – right	2.99 (0.22)	3.00 (0.30)	0.98	0.336	3.03 (0.27)	2.98 (0.27)	–0.57	0.572
Cingulate gyrus – left	3.67 (0.23)	3.61 (0.30)	0.36	0.719	3.73 (0.20)	3.61 (0.29)	–1.36	0.186
Rostral anterior cingulate – left	3.86 (0.29)	3.79 (0.34)	0.35	0.727	3.90 (0.20)	3.79 (0.35)	–1.26	0.220
Caudal anterior cingulate – left	3.47 (0.28)	3.44 (0.36)	0.31	0.757	3.54 (0.33)	3.42 (0.32)	–1.02	0.318
Cingulate gyrus – right	3.55 (0.24)	3.54 (0.20)	0.08	0.934	3.57 (0.26)	3.53 (0.20)	–0.35	0.729
Rostral anterior cingulate – right	3.87 (0.33)	3.83 (0.37)	0.65	0.520	3.94 (0.26)	3.82 (0.37)	–1.59	0.125
Caudal anterior cingulate – right	3.32 (0.35)	3.35 (0.21)	–0.44	0.667	3.31 (0.37)	3.34 (0.24)	0.96	0.344
OFC – left	3.35 (0.22)	3.40 (0.24)	1.78	0.086	3.42 (0.23)	3.36 (0.24)	–1.23	0.230
Lateral OFC – left	3.43 (0.23)	3.41 (0.26)	1.28	0.210	3.52 (0.23)	3.38 (0.24)	–1.60	0.123
Medial OFC – left	3.24 (0.25)	3.38 (0.29)	2.02	0.054	3.28 (0.24)	3.34 (0.29)	–0.30	0.768
OFC – right	3.34 (0.18)	3.38 (0.38)	1.45	0.160	3.44 (0.27)	3.33 (0.32)	–1.57	0.128
Lateral OFC – right	3.35 (0.19)	3.43 (0.35)	1.95	0.062	3.46 (0.27)	3.37 (0.30)	–1.57	0.128
Medial OFC – right	3.32 (0.24)	3.30 (0.49)	0.62	0.538	3.42 (0.28)	3.27 (0.43)	–1.23	0.231
Posterior cingulate – left	3.14 (0.15)	3.26 (0.17)	1.32	0.200	3.17 (0.14)	3.22 (0.18)	0.03	0.975
Posterior cingulate – right	3.06 (0.15)	3.14 (0.16)	1.17	0.253	3.11 (0.18)	3.10 (0.15)	–0.22	0.825
Inferior parietal lobule – left	3.16 (0.19)	3.16 (0.21)	1.22	0.233	3.26 (0.11)	3.13 (0.21)	–1.56	0.131
Inferior parietal cortex – left	3.18 (0.22)	3.15 (0.26)	0.95	0.349	3.29 (0.18)	3.12 (0.25)	–1.59	0.125
Supramarginal gyrus – left	3.15 (0.19)	3.18 (0.19)	1.43	0.166	3.24 (0.10)	3.14 (0.21)	–1.34	0.192
Inferior parietal lobule – right	3.05 (0.28)	3.04 (0.30)	1.34	0.192	3.20 (0.24)	2.99 (0.29)	–1.39	0.175
Inferior parietal cortex – right	3.16 (0.24)	3.10 (0.26)	0.37	0.714	3.24 (0.20)	3.08 (0.25)	–0.59	0.561
Supramarginal gyrus – right	2.91 (0.37)	2.96 (0.39)	1.94	0.063	3.13 (0.32)	2.87 (0.38)	–1.81	0.082
Superior temporal gyrus – left	3.17 (0.26)	3.15 (0.22)	0.78	0.440	3.30 (0.16)	3.11 (0.24)	–1.90	0.069

Region	PME				PTE			
	non-PME (n = 15)	PME (n = 20)	t value	p[1]	non-PTE (n = 9)	PTE (n = 26)	t value	p[1]
Superior temporal gyrus – right	3.13 (0.36)	3.08 (0.31)	0.76	0.452	3.29 (0.26)	3.03 (0.32)	–1.65	0.112
Post. asp. sup. temporal sulcus – left	2.99 (0.26)	2.91 (0.25)	0.12	0.905	3.13 (0.19)	2.88 (0.25)	–0.99	0.332
Post. asp. sup. temporal sulcus – right	3.11 (0.42)	2.99 (0.37)	0.99	0.332	3.37 (0.32)	2.93 (0.35)	–2.40	0.024*
Lingual gyrus – left	2.40 (0.24)	2.39 (0.19)	0.38	0.709	2.48 (0.27)	2.36 (0.18)	–0.90	0.375
Lingual gyrus – right	2.44 (0.26)	2.51 (0.19)	1.35	0.187	2.54 (0.27)	2.46 (0.20)	–1.53	0.138
Inferior temporal gyrus – left	3.27 (0.27)	3.20 (0.32)	0.62	0.543	3.40 (0.22)	3.17 (0.30)	–1.58	0.125
Inferior temporal gyrus – right	3.29 (0.28)	3.17 (0.37)	0.24	0.810	3.40 (0.31)	3.16 (0.32)	–1.11	0.279
Lateral occipital cortex – left	2.59 (0.23)	2.57 (0.18)	0.79	0.436	2.70 (0.22)	2.54 (0.18)	–1.86	0.074
Lateral occipital cortex – right	2.70 (0.19)	2.69 (0.17)	1.27	0.214	2.79 (0.20)	2.67 (0.16)	–2.13	0.043
Middle temporal gyrus – left	3.44 (0.28)	3.27 (0.31)	–0.13	0.899	3.58 (0.20)	3.26 (0.29)	–1.73	0.095
Middle temporal gyrus – right	3.28 (0.37)	3.25 (0.45)	1.20	0.241	3.52 (0.23)	3.17 (0.43)	–1.79	0.085
Parahippocampal gyrus – left	2.76 (0.35)	2.96 (0.36)	1.07	0.296	2.77 (0.27)	2.92 (0.39)	1.48	0.150
Parahippocampal gyrus – right	2.84 (0.24)	2.84 (0.34)	0.22	0.831	2.91 (0.12)	2.81 (0.33)	0.26	0.798
Inferior frontal gyrus – left	3.20 (0.19)	3.17 (0.21)	0.34	0.735	3.26 (0.19)	3.16 (0.20)	–1.17	0.252
Pars opercularis gyrus – left	3.13 (0.19)	3.13 (0.23)	0.87	0.393	3.19 (0.19)	3.11 (0.22)	–1.07	0.294
Pars triangularis gyrus – left	3.16 (0.28)	3.09 (0.24)	0.45	0.656	3.22 (0.32)	3.08 (0.23)	–1.42	0.169
Pars orbitalis gyrus – left	3.47 (0.33)	3.51 (0.35)	0.27	0.792	3.55 (0.32)	3.48 (0.35)	0.11	0.916
Inferior frontal gyrus – right	3.08 (0.23)	3.10 (0.33)	1.47	0.153	3.21 (0.22)	3.06 (0.30)	–1.59	0.124
Pars opercularis gyrus – right	3.06 (0.23)	3.05 (0.31)	1.54	0.136	3.19 (0.18)	3.01 (0.29)	–1.58	0.126
Pars triangularis gyrus – right	2.99 (0.26)	3.03 (0.34)	1.60	0.122	3.13 (0.26)	2.98 (0.31)	–1.60	0.121
Pars orbitalis gyrus – right	3.34 (0.36)	3.37 (0.47)	1.02	0.318	3.42 (0.44)	3.34 (0.41)	–0.89	0.384
Precuneus cortex – left	3.02 (0.19)	3.01 (0.19)	1.08	0.290	3.06 (0.20)	3.00 (0.19)	–1.07	0.297
Precuneus cortex – right	2.99 (0.18)	2.98 (0.16)	0.50	0.622	3.03 (0.13)	2.97 (0.17)	–0.59	0.561
Precentral gyrus – left	2.80 (0.11)	2.80 (0.20)	0.92	0.364	2.81 (0.13)	2.80 (0.18)	–0.49	0.625
Precentral gyrus – right	2.68 (0.19)	2.74 (0.27)	1.41	0.171	2.76 (0.23)	2.70 (0.24)	–0.68	0.501
Superior frontal gyrus – left	3.50 (0.18)	3.52 (0.28)	1.47	0.153	3.51 (0.21)	3.51 (0.26)	–0.90	0.377
Superior frontal gyrus – right	3.40 (0.15)	3.45 (0.28)	0.89	0.383	3.43 (0.13)	3.43 (0.26)	–0.02	0.982
Superior parietal cortex – left	2.86 (0.20)	2.80 (0.13)	0.00	0.998	2.91 (0.18)	2.79 (0.15)	–0.82	0.417
Superior parietal cortex – right	2.83 (0.20)	2.81 (0.15)	0.19	0.848	2.87 (0.18)	2.80 (0.16)	–0.32	0.753
Frontal pole – left	3.67 (0.52)	3.55 (0.65)	0.05	0.963	3.52 (0.50)	3.63 (0.63)	0.49	0.628

Region	PME				PTE			
	non-PME (n = 15)	PME (n = 20)	t value	p[1]	non-PTE (n = 9)	PTE (n = 26)	t value	p[1]
Frontal pole – right	3.57 (0.60)	3.63 (0.60)	–0.03	0.973	3.55 (0.67)	3.63 (0.57)	0.39	0.700

Values in parentheses are SD. Post. asp. sup. = Posterior aspect of the superior.

[1] Adjusted for prenatal MA (or TOB), marijuana, age at time of scan, gender, handedness and pulse sequence.

* $p \leq 0.099$ after multiplicity adjustment within domain category using the step-up Hochberg Bonferroni method [60].

Table 7

Average cortical volume of imaged participants in mm^3

Region	PME				PTE			
	non-PME (n = 15)	PME (n = 20)	t value	p[1]	non-PTE (n = 9)	PTE (n = 26)	t value	p[1]
DLPFC – left								
Rostral middle frontal – left	18,412.6 (2,542.6)	18,151.2 (3,108.2)	–0.16	0.875	18,235.3 (2,294.4)	18,272.9 (3,049.8)	–0.77	0.449
Caudal middle frontal – left	7,185.9 (1,140.7)	6,897.8 (1,105.2)	0.36	0.723	7,569.1 (800.9)	6,831.6 (1,155.3)	–1.59	0.124
DLPFC – right								
Rostral middle frontal – right	19,823.7 (3,091.0)	19,364.8 (2,432.5)	–0.20	0.842	18,596.1 (2,379.0)	19,895.7 (2,767.1)	0.37	0.713
Caudal middle frontal – right	6,515.8 (1,044.9)	6,744.8 (1,239.1)	1.46	0.157	6,928.3 (1,034.6)	6,549.1 (1,189.7)	–1.96	0.061
Cingulate gyrus – left								
Rostral anterior cingulate – left	2,513.3 (409.6)	2,617.0 (444.0)	0.69	0.499	2,408.9 (391.0)	2,629.2 (430.8)	0.38	0.704
Caudal anterior cingulate – left	2,031.7 (378.2)	2,100.4 (418.2)	0.07	0.943	2,023.1 (425.3)	2,087.5 (394.6)	–0.41	0.689
Cingulate gyrus – right								
Rostral anterior cingulate – right	2,012.3 (369.1)	1,890.4 (381.6)	1.12	0.273	2,048.7 (433.1)	1,906.0 (355.8)	–2.02	0.054
Caudal anterior cingulate – right	2,307.3 (649.3)	2,331.1 (494.3)	0.40	0.689	2,352.3 (779.4)	2,310.0 (476.6)	–0.33	0.743
OFC – left								
Lateral OFC – left	8,915.1 (713.6)	8,539.0 (1,248.6)	0.00	0.998	8,901.9 (711.6)	8,630.4 (1,156.2)	–0.21	0.834
Medial OFC – left	5,376.9 (715.5)	5,608.7 (993.2)	0.91	0.370	5,299.9 (886.3)	5,581.8 (884.5)	0.09	0.926
OFC – right								
Lateral OFC – right	8,631.5 (739.7)	8,054.9 (943.4)	–0.38	0.707	8,868.6 (726.5)	8,105.9 (878.9)	–1.37	0.183
Medial OFC – right	5,711.7 (601.9)	5,949.5 (1,384.0)	0.57	0.575	5,666.6 (646.0)	5,910.3 (1,236.3)	–0.09	0.926
Posterior cingulate – left	3,879.1 (423.2)	4,119.5 (424.9)	0.45	0.657	3,923.6 (482.8)	4,048.6 (422.5)	–0.05	0.964
Posterior cingulate – right	4,003.1 (668.2)	4,000.8 (587.7)	0.06	0.952	3,962.3 (767.3)	4,015.5 (568.6)	0.16	0.874
Inferior parietal lobule – left								
Inferior parietal cortex – left	16,717.7 (2,328.8)	15,205.3 (2,009.8)	–1.05	0.305	16,581.0 (1,741.5)	15,601.7 (2,380.0)	–0.09	0.931
Supramarginal gyrus – left	14,224.9 (1,799.1)	13,943.0 (1,789.2)	1.07	0.296	14,797.8 (1,064.0)	13,809.7 (1,910.3)	–1.37	0.184
Inferior parietal lobule – right								
Inferior parietal cortex – right	20,174.9 (2,270.8)	18,978.7 (1,820.8)	–0.38	0.709	20,580.8 (2,423.6)	19,114.2 (1,855.5)	–0.84	0.407
Supramarginal gyrus – right	11,996.5 (1,798.0)	11,885.1 (1,834.8)	1.68	0.106	12,668.3 (2,079.9)	11,678.2 (1,651.3)	–1.37	0.182
Superior temporal gyrus – left	13,252.0 (1,280.2)	12,671.1 (1,910.7)	0.19	0.848	13,365.1 (1,132.0)	12,766.0 (1,817.1)	–1.38	0.180

Region	PME				PTE			
	non-PME (n = 15)	PME (n = 20)	t value	p[1]	non-PTE (n = 9)	PTE (n = 26)	t value	p[1]
Superior temporal gyrus – right	12,939.7 (1,640.0)	11,833.4 (2,037.0)	–0.70	0.493	13,418.6 (1,582.2)	11,922.9 (1,918.4)	–1.75	0.093
Post. asp. sup. temporal sulcus – left	3,379.0 (548.2)	2,878.2 (454.0)	–1.32	0.199	3,292.3 (518.8)	3,023.8 (552.7)	0.81	0.428
Post. asp. sup. temporal sulcus – right	3,421.7 (745.3)	2,814.3 (593.8)	–2.51	0.019*	3,141.9 (535.5)	3,051.3 (782.0)	0.73	0.474
Lingual gyrus – left	7,391.2 (896.3)	6,882.2 (1,062.5)	–1.33	0.195	7,376.1 (572.6)	7,004.9 (1,120.2)	–0.06	0.953
Lingual gyrus – right	7,469.5 (726.2)	7,504.9 (1,314.5)	0.03	0.976	7,348.7 (733.0)	7,538.5 (1,194.7)	0.36	0.722
Inferior temporal gyrus – left	11,732.7 (2,042.2)	10,252.1 (1,604.6)	–1.35	0.191	12,137.8 (1,526.8)	10,453.5 (1,881.3)	–1.14	0.263
Inferior temporal gyrus – right	10,524.5 (2,405.7)	10,176.9 (2,362.5)	–0.06	0.956	10,814.4 (2,388.5)	10,156.7 (2,362.8)	–0.18	0.861
Lateral occipital cortex – left	14,479.3 (1,595.2)	13,965.7 (2,294.8)	0.17	0.869	14,860.6 (1,822.9)	13,952.2 (2,057.6)	–0.94	0.355
Lateral occipital cortex – right	13,548.5 (1,655.6)	13,103.0 (1,795.1)	–0.88	0.389	13,432.1 (1,865.7)	13,246.1 (1,711.4)	–0.59	0.561
Middle temporal gyrus – left	13,143.5 (1,105.2)	11,603.8 (1,848.5)	–1.18	0.249	13,569.2 (1,038.8)	11,811.7 (1,709.5)	–1.05	0.303
Middle temporal gyrus – right	13,281.9 (1,873.4)	12,225.3 (2,560.3)	–0.18	0.861	13,654.2 (1,964.1)	12,340.2 (2,373.6)	–0.48	0.633
Parahippocampal gyrus – left	2,230.5 (386.6)	2,222.3 (497.3)	0.60	0.555	2,311.6 (398.3)	2,196.1 (466.2)	0.14	0.892
Parahippocampal gyrus – right	2,129.9 (311.3)	2,162.2 (321.9)	0.55	0.589	2,109.1 (393.2)	2,161.9 (288.3)	0.31	0.757
Inferior frontal gyrus – left								
Pars opercularis gyrus – left	6,038.2 (677.2)	5,808.8 (711.9)	–0.02	0.984	6,123.6 (692.5)	5,832.2 (695.6)	0.06	0.951
Pars triangularis gyrus – left	4,539.4 (969.9)	4,693.8 (977.7)	0.50	0.619	4,682.7 (1,059.9)	4,608.6 (948.9)	–0.08	0.941
Pars orbitalis gyrus – left	2,615.7 (368.3)	2,545.7 (503.3)	–0.27	0.791	2,531.8 (323.8)	2,590.9 (485.5)	0.90	0.379
Inferior frontal gyrus – right								
Pars opercularis gyrus – right	4,486.1 (862.6)	4,958.4 (745.7)	1.86	0.074	4,761.6 (1,123.5)	4,754.0 (715.4)	–1.41	0.171
Pars triangularis gyrus – right	5,444.4 (900.3)	5,293.2 (1,160.7)	0.21	0.838	5,244.6 (831.2)	5,397.3 (1,121.8)	0.44	0.665
Pars orbitalis gyrus – right	3,014.1 (436.3)	3,125.4 (577.5)	0.86	0.400	3,154.3 (446.5)	3,051.2 (545.6)	–1.00	0.329
Precuneus cortex – left	12,247.0 (1,332.4)	11,884.8 (1,592.9)	0.38	0.708	12,094.1 (1,268.8)	12,021.3 (1,557.8)	0.21	0.838
Precuneus cortex – right	12,652.2 (1,415.0)	11,890.8 (1,548.1)	–0.65	0.522	12,623.4 (1,671.8)	12,076.4 (1,472.1)	–0.01	0.992
Precentral gyrus – left	13,914.5 (1,267.2)	13,948.1 (1,188.3)	0.56	0.579	13,500.9 (708.7)	14,083.5 (1,312.0)	0.56	0.583
Precentral gyrus – right	13,581.5 (1,255.6)	13,533.5 (1,817.2)	0.92	0.365	13,873.2 (1,250.5)	13,443.5 (1,686.3)	–1.02	0.317
Superior frontal gyrus – left	26,225.1 (2,757.5)	26,086.5 (2,989.8)	0.82	0.421	26,385.1 (3,520.6)	26,063.0 (2,657.9)	–1.28	0.213
Superior frontal gyrus – right	25,502.2 (2,557.9)	25,810.3 (2,695.3)	0.40	0.690	25,468.1 (2,634.1)	25,751.0 (2,641.2)	–0.23	0.818
Superior parietal cortex – left	16,920.1 (2,503.9)	16,461.7 (2,243.9)	0.13	0.898	17,026.6 (2,397.9)	16,530.7 (2,346.0)	–0.24	0.809
Superior parietal cortex – right	16,751.5 (1,512.2)	17,303.1 (1,907.7)	0.38	0.709	16,842.8 (1,371.2)	17,144.2 (1,877.4)	0.70	0.490
Frontal pole – left	1,021.1 (248.5)	987.0 (303.1)	–0.64	0.527	909.3 (218.6)	1,033.5 (292.2)	1.90	0.069

Region	PME				PTE			
	non-PME (n = 15)	PME (n = 20)	t value	p[1]	non-PTE (n = 9)	PTE (n = 26)	t value	p[1]
Frontal pole – right	1,306.0 (335.8)	1,375.1 (454.6)	–0.07	0.945	1,240.4 (216.5)	1,381.8 (448.9)	0.68	0.503

Values in parentheses are SD. Post. asp. sup. = Posterior aspect of the superior.

[1] Adjusted for prenatal MA (or TOB), marijuana, age at time of scan, gender, handedness, pulse sequence and total intracranial volume.

* $p \leq 0.099$ after multiplicity adjustment within domain category using the step-up Hochberg Bonferroni method [60].